

Defects in Nonceramic Insulators: Can They be Detected in a Timely Manner?

*S. Gorur and S. Sivasubramaniyam Department of Electrical Engineering,
Arizona State University, Tempe, AZ, USA*

This work was performed under a PSERC (Power Systems Engineering Research Center) funded project at Arizona State University

Abstract: This paper is a continuation of the work reported during the 2004 Daycor users meeting. The electric field measurement method has been explored to determine its potential for timely detection of defects in nonceramic insulators. Various types of defects were simulated and the external electric field was computed. It is shown that the electric field method used presently is not sensitive enough to permit early detection of defective. There is a need for an improved method, perhaps periodic corona inspection could be the answer.

Introduction: There are a multitude of designs, materials, formulations, and manufacturing processes that are used presently for nonceramic insulators. While this beneficial in terms of offering choices for the users, this also means that in case of problems, failure patterns could be different. It is fairly well known that most problems in NCI result originate from interfaces. The critical interfaces in this type of insulator are between the rod and housing, between hardware-rod-housing and different sheds of housing if unit is not manufactured in a single piece.



Fig.1: NCI Line Post that was removed from service in Southern USA

The presence of corona at the interfaces leads to sheath damage exposing the fiberglass rod, tracking the rod, thereby leading to insulator failure through interfacial flashover, rod burning and brittle fracture. Also, the presence of any contamination like water, salts, and dirt can intensify the field at those locations. Fig. 1 shows a picture of a failed NCI. It can be seen that the first few sheds have suffered corona cutting. Some degradation in the form of tracking and erosion is also visible. If the damage to the insulator is not in the line of sight, then this may not be identified as a problem during routine line inspection by road or helicopter patrols until the unit fails. The challenge is to identify such insulators at an early stage of degradation when there is still time to act.

Understanding the electric field distribution plays a vital role in insulator design and also can be useful for detecting internal defects. In ceramic insulators the voltage distribution is relatively more linear due to the presence of intermediate metal parts. The material does not degrade with corona, hence corona is not

usually a problem in ceramic insulators. However in NCI's the voltage distribution is highly non-uniform as shown in Fig. 2, and can give rise to corona. Corona rings are normally used for NCI at voltages above 230 kV in order to reduce the electric field near the line end.

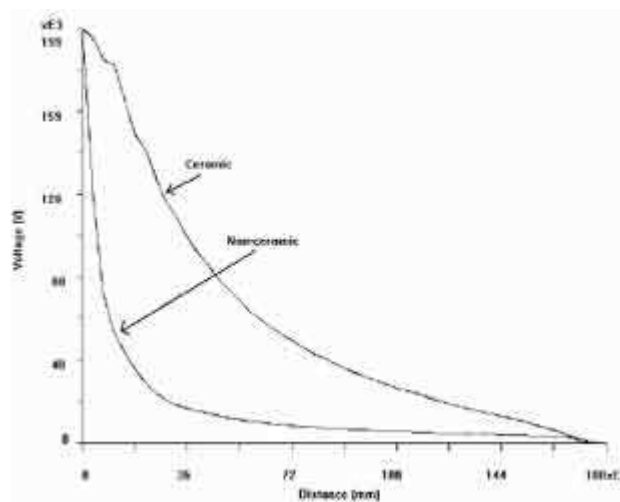


Fig.2: Significant difference in the voltage distribution exists between ceramic and NCI due to differences in construction. The insulator modeled is a 345 kV insulator

There have been several recent publications that concluded that there is no fool-proof method for early detection of defects in nonceramic insulators. Among the methods examined were partial discharge detection, infrared thermography, corona and audible noise detection, leakage current measurement and electric field measurement [1]. In the utility environment the electric field technique is being increasingly used as a diagnostic tool to identify defective porcelain units [2, 3]. Their use on nonceramic insulators appears to be the logical step. What types and degrees of defects can be detected by such a measurement? This study was undertaken to answer this question. The electric field distribution of a healthy insulator was taken as the reference. Types of Defects Modeled: Several types of defects that can occur on a NCI were modeled. The various types of defects that are considered difficult to detect but critical are incorporated on to the healthy model and simulated. The size, position and conductivity of such defects are varied. The field values for locations close to the defect along the path of the probe are noted down. These values are then compared with the values obtained in the healthy cases. The presently used electric field probes are sensitive for field values above 2 kV/m [2]. Hence defects that produce a difference of 2 kV/m and above are considered detectable while others were considered undetectable. The differences in field values thus obtained are plotted as a function of the shed number. A logarithmic trend line is fitted to the above plot for a better perception of the defect detection possibilities.

Various types of defects such as those occurring on the shed, shank, interface, external tracks from end fittings and tracks occurring on the rod sheath interface were considered. Most of the external defects could be observed during careful

visual inspection. However, defects that occur inside the housing are not visible. Hence such defects are modeled for electric field distortion studies to verify the possibility of detecting such defects using field probes as shown in Table 1. A defect that occurs for the distance between any two consecutive sheds is named as the single shed defect. A single shed defect will have the shape of a cylinder with a 9.2 cm height and 5 mm diameter. A diagrammatic representation of various types of single shed defects modeled is as shown in Fig. 3. Similarly two-shed and three shed defects are simulated and analyzed.

Table 1: Various Defects Modeled in Non-Ceramic Insulators

Defect Type	Description
Single shed defect	Fully conductive defect at rod sheath interface 100 mS/m conductive water defect at rod sheath interface Air void defect at rod sheath interface
Two shed defect	Fully conductive defect at rod sheath interface 100 mS/m conductive water defect at rod sheath interface Air void defect at rod sheath interface
Three shed defect	Fully conductive defect at rod sheath interface 100 mS/m conductive water defect at rod sheath interface Air void defect at rod sheath interface

Table 1: Various Defects Modeled in Non-Ceramic Insulators

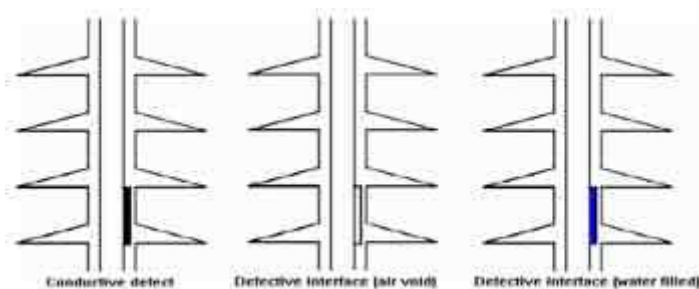


Fig.3: Diagrammatic representations of various types of defects modeled. A defect of 1 shed spacing is taken as the minimum length of the defect. The length of the defects were increased to span 2 and 3 sheds

The field calculations are performed on the insulator along the axis as indicated by the path AB in Fig. 4. A distance of 2mm is assumed for the air gap in order to slide the probe on the insulator. The values obtained are compared with that of a healthy insulator and the change in field value is plotted against the shed number. The data for a defect of lengths equal to 1 shed spacing and 2 shed spacing are shown in Figs. 5 and 6.

It can be seen that the possibility of detecting defects in close proximity to the HV electrode is good, irrespective of the defect type. However, should the location be towards the middle of the insulator or towards the ground end, their chances of being detected is small or zero.

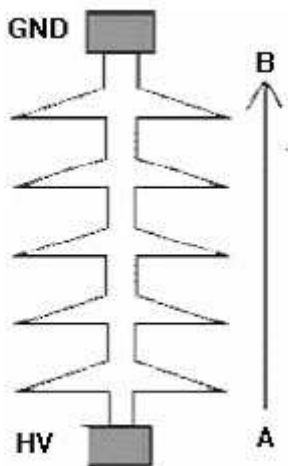


Fig.4: Measurement along insulator surface from location A to B. The line AB is about 2 mm away from the tip of the shed to permit probe movement

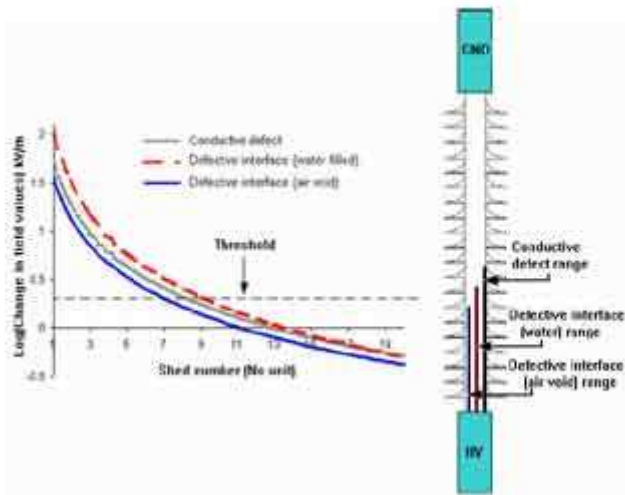


Fig.5: Range of detectability for defects that of length= 1 X shed spacing. Probe is assumed to me in the axial direction AB

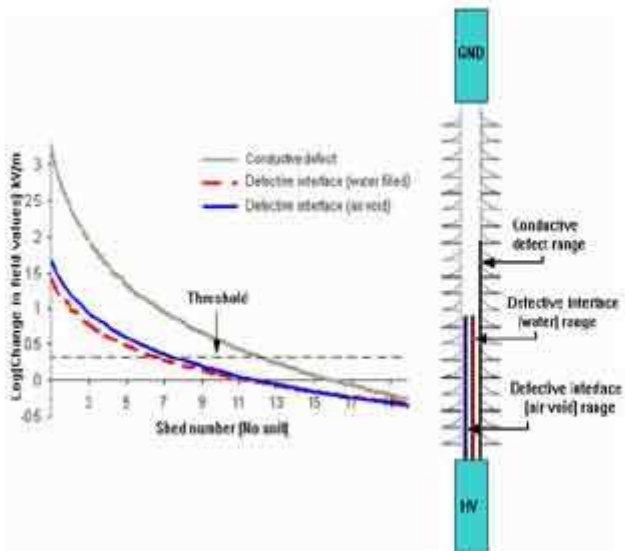


Fig. 6: Range of detectability for defects that of length= 2Xshed spacing. Probe is assumed to me in the axial direction AB

It is clear that in order to be able to detect any defect it is important to get as close as possible to the origin of the defect. As an illustration if it were to be possible to measure the electric field at the point C, Fig. 7, (2 mm away from the shank) then as is shown in Fig. 8, most defects can be detected irrespective of their location along the insulator. Can this be achieved in practice is a good question.

It is likely that corona cuts or any other deformities in the insulator will give rise to corona, especially under humid conditions. The work reported last year showed that a combination of location specifics and quantitative data like brightness can provide useful information on making decisions such as problematic corona or nonproblematic corona. This should be explored further.

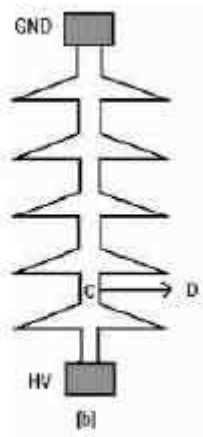


Fig.7: Measurement in radial direction from C to D. The point C is about 2 mm away from the sheath

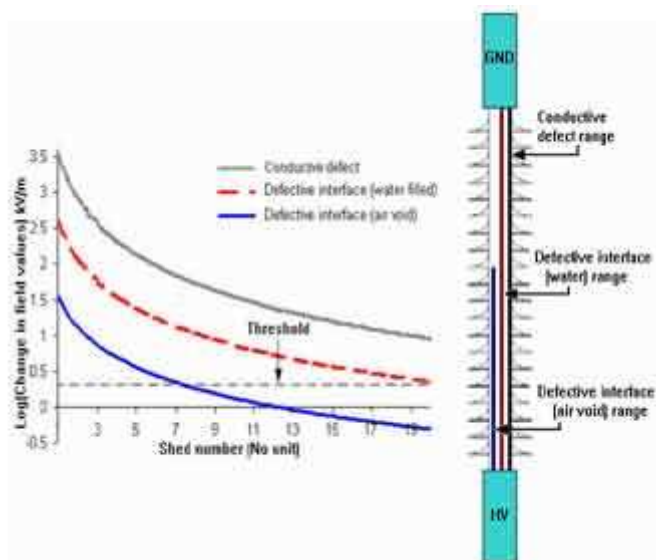


Fig.8: Range of detectability for defects that of length= 1 X shed spacing. Probe is assumed to be in the radial direction and is closest to point C

Conclusions:

The defect detection is position dependant and has the best possibility of being detected if it is closer to the high voltage electrode.

Larger and longer defects produce higher field changes hence they are more easily detected than the smaller ones.

The change in field value observed depends on the type of the defect. More conductive the defect is, greater is the possibility of detecting it.

The range of the field probe can be greatly enhanced if measurements are taken radially instead of conventional axial measurements.

References:

- [1] IEEE task force on electrical testing of polymer insulators for hot line installation, "Electrical test methods for non-ceramic insulators used for live line replacement," IEEE Trans. Power Delivery, vol. 12, no. 2, pp. 965-970, April 1997.
- [2] G. H. Vaillancourt, J. P. Bellerive, M. St-Jean, and C. Jean, "New live line tester for porcelain suspension insulators on high voltage power lines," IEEE Trans. Power Delivery, vol. 9, no. 1, pp. 208-219, Jan. 1994.
- [3] G. H. Vaillancourt, S. Carignan, and C. Jean, "Experience with the detection of faulty composite insulators on high voltage power lines by the electric field measurement method," IEEE Trans. Power Delivery, vol. 13, no. 2, pp. 661-666, Apr. 1998.

Transmission Line Insulator Condition Monitoring

David Stuart McLennan – SP AusNet

Abstract: Transmission line insulator condition monitoring is of increasing interest with the ageing of many transmission lines constructed since the 1950s. Porcelain and toughened glass and more recently polymeric insulators all have characteristic degradation and pollution modes that must be considered by asset managers. Following the recent inspection of some 220 kV Transmission Line Insulators it is useful to summarise current understanding of ceramic insulator degradation and condition assessment.

A number of technical papers indicate that porcelain insulators degrade with time and applied electrical and mechanical stress. The electrical stress applied to a suspension insulator string is not uniform with the highest stress occurring close to the live conductor. An AEP study of 1100 service aged porcelain disc insulators came to the following conclusions:

- Porcelain punctures occur in the region of maximum electrical stress between the metal cap and the pin.
- Long-term high electrical stress affects the electrical properties of the insulator porcelain over time.
- Insulation resistance tests support the tendency of a reduction in dielectric strength under high electric stress.
- Manufacturing variations may lead to localized high stress concentrations in individual insulators.

SP AusNet experience supports the tendency for degradation to be more common at the higher stress string positions close to the conductor. Manufacturing variations however would explain the more random string location of degraded insulators that is also observed. There are a number of possible degradation mechanisms and a number of manufacturing issues that are believed to influence degradation.

Insulator Mortar Cement Growth

The cement composition used in insulators to bond the porcelain and pin inside the cap influences the volume expansion or contraction over time. Cement expansion can place a mechanical hoop stress on the porcelain that leads to radial cracking. This tends to be a batch issue. Interface stresses can also occur at the cement-porcelain and cement metal interfaces.

Pin Corrosion

Pin corrosion also limits the mechanical life of porcelain insulator strings. The extent of corrosion is normally determined visually and by sampling, mechanical testing and measurement of material loss. Volume expansion of rust products inside the porcelain has been proposed as another source of porcelain radial cracking. Zinc sleeves and other modifications have been adopted in improved designs to delay the occurrence of pin corrosion.



Figure 1 Section view of a porcelain insulator

Porcelain Micro-Cracking

Porcelain material and component manufacturing imperfections including voids can lead to the formation and growth of micro-cracks in the porcelain. Thermal cycling and differential thermal expansion between materials and the applied electrical and mechanical stress grow these cracks, which may develop into carbonised conducting channels between the metal pin and cap. This produces a lower insulation resistance and increased dielectric losses and heating in this disc. Electrical stress is highest near the conductor so it is common for the insulator closest to the conductor to be in a degraded condition. However, degradation also depends strongly on manufacturing imperfections that tend to create stress concentration points, therefore random failures can occur at any position in the string.

Glass Insulator Degradation

Loss of mechanical strength through pin corrosion also limits the mechanical life of glass insulator strings. The extent of corrosion is again determined visually and by sampling, mechanical testing and measurement of material loss. Toughened glass insulators do not appear to have a gradual insulation degradation path and are generally accepted to be either broken or good. Glass insulators are designed to maintain high mechanical performance even when the glass sheds have been shattered. Surface pollution, pin corrosion and shed integrity are the main condition monitoring concerns with glass insulators.



Figure 2 Shattered glass insulator with corroded pin

Non-Ceramic Insulator Degradation

Polymeric insulators have been reported with a range of failure modes. Hydro-Quebec has reported a close correlation between electric field strength variations and surface temperature caused by faults in polymeric insulators. Hydro-Quebec conclude that their electric field measurement method is effective in both laboratory and substation locations. They report that infrared cameras are effective in the laboratory but they had interpretation difficulties in a substation. Infrared can be difficult to interpret when the field of view is cluttered with other equipment giving thermal signatures or if solar reflections are visible.

SP AusNet's practice is to inspect lines when the sky is completely overcast or at night to remove the solar reflection or solar heating effects. Overhead insulators inspected from the ground against a uniform temperature sky are also clear from interference. It is expected that corona and infrared will be effective inspection tools for polymeric insulators but we do not have survey results at this time.

Insulator Pollution

In damp conditions a partially conducting layer of pollution on an insulators surface can increase surface leakage currents and cause surface heating and dry-band arcs. Higher pollution levels lead to eventual flashover of the insulator string. Insulators are designed to withstand a reasonable level of pollution under normal service conditions however environmental factors can lead to an unacceptable level building up over time. A variety of conducting materials may pollute an insulator's surface. In coastal regions salt spray may be deposited by the wind. In the vicinity of major roads and industrial areas various chemical products may be deposited and near quarries or dry areas dust may build up. The deposition of these films may be fairly random depending on weather and climate variations over time. This brings an element of uncertainty into the scheduling and effectiveness of remedial programs such as periodic washing.

Ceramic Insulators

Pollution flashover is affected by the nature of the insulators surface. Ceramic insulators are said to be hydrophilic meaning that the surface wets completely under heavy fog or rain conditions. With the presence of deposited salts a conducting electrolyte film may cover the insulator surface partially or completely. If the surface is covered completely increased leakage currents can flow heating the surface and drying some areas. Dry bands may form interrupting the flow of current and distorting the voltage field. The dry bands may flashover and if the resistance of the conducting film is low, eventually bridge the complete insulator string. In humid conditions pollution build-up on the lower surface of ceramic suspension insulators can result in a moist conductive layer being formed that tends to equalize the voltage across this lower surface. The voltage drop is then mostly across the cleaner upper surface. This results in an increased intensity of the voltage field on the top surface and an increase in the shed dielectric and surface heating. The probability of external insulator flashover increases for this condition. This condition can be detected by infrared or corona camera.

Polymeric Insulators

There is an extensive literature on pollution of non-ceramic insulators. Polymeric insulators may suffer loss of hydrophilic surface condition as they age and corona and arcing can seriously damage the insulator surface. Corona cameras and infrared cameras are effective in detecting these problems.

Pollution Modeling

There are many mathematical models for pollution modeling that may be used to study insulator performance. A simple model [9] for the flashover process of a polluted insulator is a conducting pollution layer in series with a partial arc spanning a dry band region. Where (ra) is the resistance per unit length of the arc and (rp) is the resistance per unit length of the pollution layer, the expression for the voltage applied across the insulator is

$$V = I * (ra * x + rp * (L-x)) \quad (1)$$

Where: I is the leakage current; X is the length of the arc; L is the total leakage distance of the insulator

The resistance per unit length (ra) can be expressed as

$$ra = A * I - (n+1) \quad (2)$$

Where: A and n are arc constants

The resistance of the pollution may be expressed as

$$rp = l / (PI * Deq * sc) \quad (3)$$

Where: l is the per unit length; Deq is the equivalent insulator diameter; sc is the surface

conductivity

Surface conductivity can be expressed in terms of equivalent salt deposit density C (ESDD) by

$$sc = (369 \cdot C + 0.42) \cdot 10^{-6} \quad (4)$$

Where: C is the Equivalent Salt Density Deposit (ESDD)

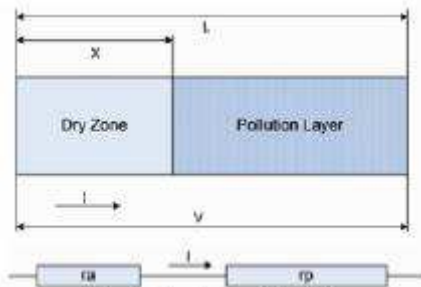


Figure 3 Simplified equivalent circuit

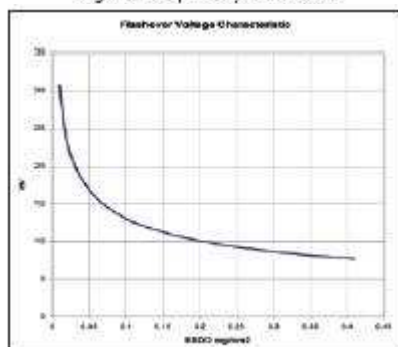


Figure 4 Insulator flashover characteristic



Figure 5 Glass insulator string

Equivalent salt Density Deposit

ESDD is the amount of common salt (NaCl) deposit that has the same conductivity as the insulator pollution deposit dissolved in the same volume of water. ESDD is the method that is commonly used in standards and by researchers for comparisons between insulator tests and models. Computer studies and experimental results show that a typical characteristic for flashover voltage versus pollution density (ESDD) is of the form shown in Figure 4. This graph (Figure 4) shows why the electrical stress ageing is more intense close to the conductor. It appears that the strong electrical field in this region and the rain wash-down effect also encourages greater pollution deposition on the lower insulator units.

fault Detection

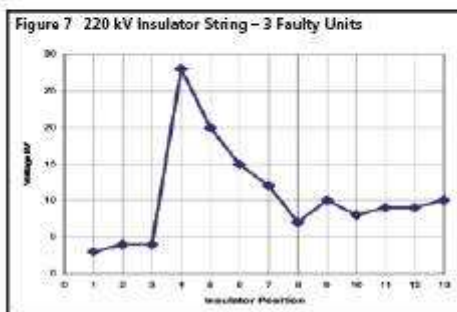
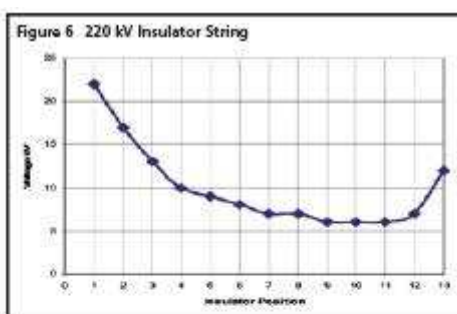
Faulty porcelain insulators have some degradation modes that are impossible to detect by visual inspection. Degradation caused by internal cracking may be detected if the insulation resistance has dropped sufficiently to distort the applied electrical field.

The field is weak across the defective insulator and high on the next good insulator. The test methods normally used to detect faulty insulators are: Voltage detection or

measurements across each insulator live I (see Figure 6 and Figure 7). Resistance measurement (Megger) of each insulator de- ii energised. Electric field measurement near each live insulator. iii

Note: These 3 methods require physical access to the insulators and for the insulators to be relatively clean and the humidity to be less than 70%. Non-invasive remote inspections using corona cameras and iv infrared cameras.

The high field on the first good insulator after a low resistance insulator may be detected by an increase in corona using the corona camera and an increase in the temperature of the insulator above ambient using an infrared camera (about 3-5 ÷C above ambient). For SP AusNet the definitive confirming test (method 1) is to wash the insulators and then measure and plot the voltage across each one. The voltage curve should be fairly smooth (see Figure 6) and evenly distributed for insulators in good condition. If the corona camera and infrared camera detect a problem on a glass insulator it is almost certainly pollution problem.



Interpretation of Corona and Infrared Indications

If a corona camera and an infrared camera detect a high field on a porcelain string it may be caused by adjacent faulty insulators or by pollution. Very high intensity corona on one or two insulators is more likely to indicate faulty insulators causing a highly distorted electric field (see Figure 7 and Figure 8). Whereas pollution is more likely to produce a symmetrical situation i.e. light corona on many strings on the tower especially at the live end. Visual inspection with high- magnification stabilised binoculars can help identify a high pollution situation. The infrared image shown in Figure 9 is of an insulator string with two bottom units having low resistance with cracks in the porcelain. The bottom unit has a “hot” metal cap probably due to resistance heating through the body of the porcelain. The second unit is “cold” with a low resistance crack though the porcelain. The third unit is in good condition and has lower surface heating due to surface leakage currents created by the strong electrical field.

Non-Invasive Inspection Guidelines

The following are some guidelines used internally by SP AusNet for non-invasive inspection of transmission tower insulators.

- Inspections should be carried out without interference from solar heating or

reflection and in low wind conditions. That is under overcast conditions or at night-time. Evenings and early mornings are ideal.

- Inspections should be carried out when the humidity is above 55% to ensure there is some surface leakage current and corona activity.
- Use a hand held weather station to ensure conditions are suitable and record the temperature, wind speed and relative humidity.
- Inspections should not be carried out when the insulators are wet as this high conductivity condition tends to cause voltage equalisation across the string and masks the defective units.
- Use a video recorder to capture the video output of the corona and infrared cameras.
- Use a set gain level on the corona camera for recordings to ensure ease of comparison between fault cases. The gain level can be dropped during initial investigations to find the source location.
- Use a manual setting on the infrared camera adjusted to a span of about $8\pm^{\circ}\text{C}$ around the insulator ambient temperature.
- Record the tower identification and physical arrangement in a standard manner to ensure correct identification by field groups.

Conclusion

Transmission line insulator condition monitoring is being supplemented by non-invasive methods that increase the efficiency of the inspection process. There is an ageing population of ceramic insulators that require increasing surveillance. Traditional test methods are not suitable for the new one-piece polymeric insulators but the noninvasive methods are reported as being effective.



Figure 8 Corona caused by adjacent faulty insulators

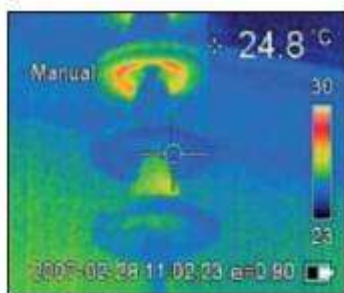


Figure 9

Effect of Corona on Nonceramic Insulator Housing Materials

B. Pinnangudi and R. S. Gorur Department of Electrical Engineering, Arizona State University, Tempe, AZ

Abstract: This paper presents results and analysis of corona studies performed on NCI removed from service as well as on new materials in the laboratory. It has been shown that it is possible to quantify the corona degradation and this could be used to answer important questions like remaining life. The approach can also be used to develop a rapid screening method for evaluating the corona resistance of materials used for NCI housings.

Introduction: Corona discharges can be a significant threat to the integrity of nonceramic insulators (NCI) due to the organic nature of the housing material [1]. For transmission class insulators (69 kV and above), corona can be a problem not only in contaminated but in clean environments as well. From worldwide experience it has been identified that a majority of NCI applications are under relatively clean or lightly contaminated conditions. On NCI, corona can be present locally for long periods of time due to inadequate hardware design, damaged hardware, and deficient interfaces due to improper design and/or manufacturing. Field inspections on 230 kV and 500 kV insulators confirm the existence of corona even under relatively dry and clean conditions [2]. In practical high-voltage systems it is difficult to avoid corona in the field, especially under wet and contaminated conditions [3, 4]. Hence, knowledge of the corona discharge magnitude and damage threshold of the housing material is essential. Corona is responsible for multiple effects such as mechanical, due to the impingement of charged particles, ultraviolet (UV) radiation, and liberation of ozone. Highly oxidizing and hydrated species of nitrogen oxides are generated which on dissolving in moisture leads to the formation of acids [5, 6]. Any cracks in the housing can expose the fiberglass core to moisture. The exposed rod can fail by tracking, erosion or brittle fracture [7, 8, 9], leading to premature failure. Hence, there is a necessity to periodically inspect NCI and replace degraded insulators in a timely manner.

Characterization of Degraded Polymers :

(i) Fourier Transform Infrared (FTIR) Spectroscopy

FTIR is a powerful tool for identifying different types of chemical bonds in organic materials [10]. Molecular bonds vibrate at various frequencies depending on the elements and the type of bonds. For a given bond, there are several specific frequencies at which it can vibrate. The wavelength of the light absorbed by the material is characteristic to the chemical bond and the strength of absorption is proportional to the concentration of the bonds [11].

(ii) Laser Treatment

The current interest in the use of lasers both for scientific investigations and for industrial applications is directly linked to the unique properties of laser light. The high spatial coherence achieved with lasers permits extreme focusing and directional irradiation at high energy densities. The monochromaticity of the laser light, together

with its tenability, opens up the possibility of highly selective narrow-band excitation [12].

The interaction mechanisms between laser light and matter depend on the parameters of the laser beam and the physical and chemical properties of the material. Laser parameters are the wavelength, intensity, spatial and temporal coherence, polarization and the angle of incidence. The material is characterized by its chemical composition and microstructure which determine the type of elementary excitations and the interactions between them. Conventional laser processing is mainly performed with IR laser light. This can excite the free electrons within the metal or vibrations within the insulator. In general the excitation energy is dissipated in the form of heat within a time which is short in comparison to any other time involved in the process. As a consequence with low and medium intensities, the laser beam can just be considered as a heat source which induces a temperature rise on the surface and the bulk of the material [13, 14, 15]. This is schematically shown in Fig. 1.

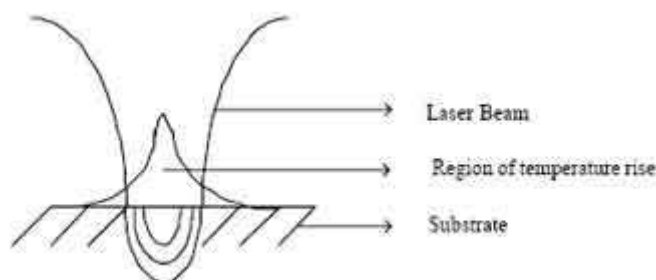


Fig 1: Heat treatment with laser

The temperature distribution is determined by the thermal and optical properties of the material. When the laser intensity (I) reaches a critical value (I_v) beyond which there is a significant material vaporization, a vapor plume is formed as shown in Fig. 2.

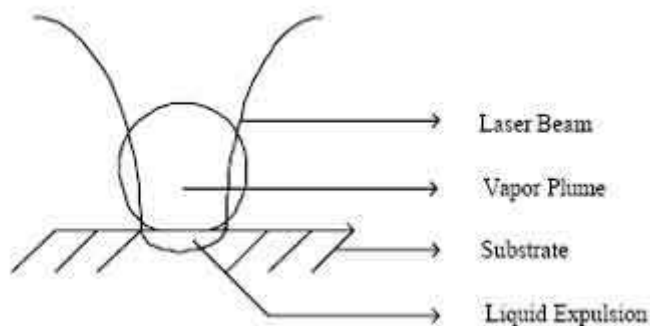


Fig 2: Heat treatment of the material with laser ($I > I_v$)

With further increase in intensity, the number of species within the plume increases and interactions between the laser and the vapor becomes very important. These result in the ionization of the species. The vapor can also be appropriately denoted as plasma [16, 17, 18].

Results and Analysis

(i) Silicone Rubber

A silicone rubber sample was subjected to corona exposure for 500 hours. A brass rod with a point tip (approximately 0.02 cm) energized by an ac voltage served as the corona source (point-plane electrode configuration). The electrode arrangement was

enclosed in an acrylic chamber with dimensions 45cm x 45cm x 120cm. Corona activity was monitored by using an oscilloscope (Tektronix model 540C) and a corona camera. Corona induced degradation was quantified by visual changes on the material surface, optical microscopy, FTIR spectroscopy and laser treatment techniques. The FTIR spectroscopic analysis was performed with a Nicolet Magna-IR 560 spectrometer equipped with an ATR device (spectra-tech model PN-0048). The corona test setup is shown in Fig. 3.

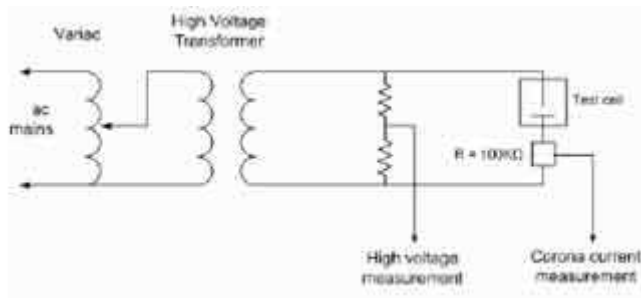


fig 3 a

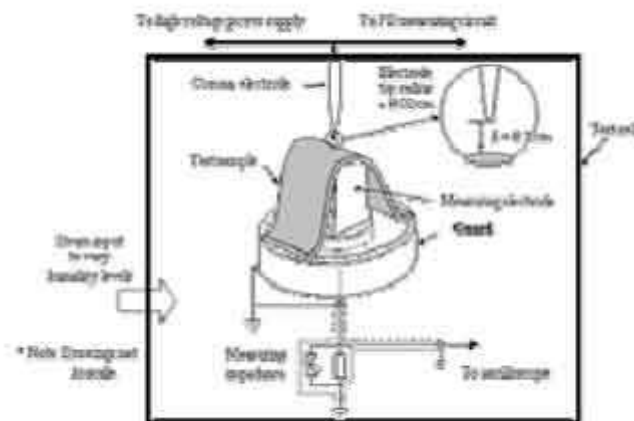


fig 3 b

Figure 3. Experimental setup to access corona performance

The sample was removed at periodic intervals to visually monitor changes on the material surface. Additionally, leakage current measurements were taken to access the corona performance of the silicone rubber sample. To determine changes at the microscopic level, if any, FTIR analysis was performed on the corona exposed region and compared with that of the virgin material. To reduce any variation in the data collected, the average of a number of spectrums (five in this study) was used. The variability reduces by a factor of \sqrt{n} , where n is the number of spectrums selected [19]. The FTIR spectrums are shown in Fig. 4.

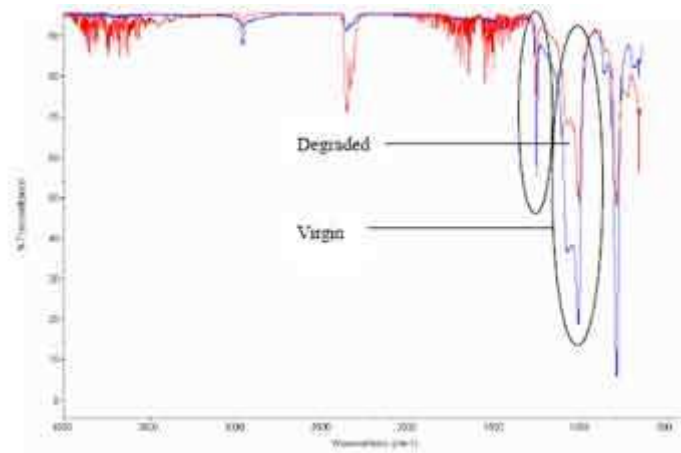


Figure 4. FTIR s spectrum of the sample before/after corona exposure

The absorption peaks corresponding to wave-numbers 1010 cm^{-1} [Si-O-Si] and 1376 cm^{-1} [-CH₃] are used as indicators for degradation. It is clear from Fig. 4 that the corona exposed region has deteriorated significantly.

The FTIR spectroscopy is a surface analysis technique. The depth/region of analysis is limited to a few microns below the sample surface. The silicone rubber material is known to regenerate /recover with time by diffusion of low molecular weight polymer chains to the surface. The technique is hence unsuitable for quantifying changes in the bulk of the material. The recovery effect in silicone rubber is shown in Fig. 5. The absorption peaks corresponding to Si-O-Si and -CH₃ are identical unlike the earlier case shown in Fig. 4.

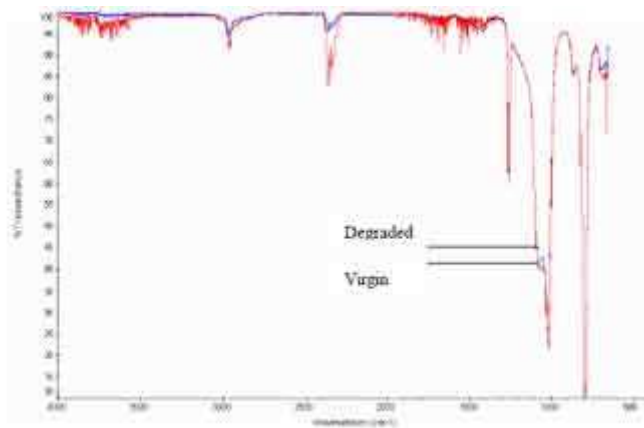


Figure 5. FTIR spectrum of the sample before/after corona exposure and recovery

The corona exposed region and the virgin sample were treated with a 1.75 watts 532 nm double YAG laser radiation for a constant time (120 seconds). The experimental setup for laser treatment is shown in Fig. 6.

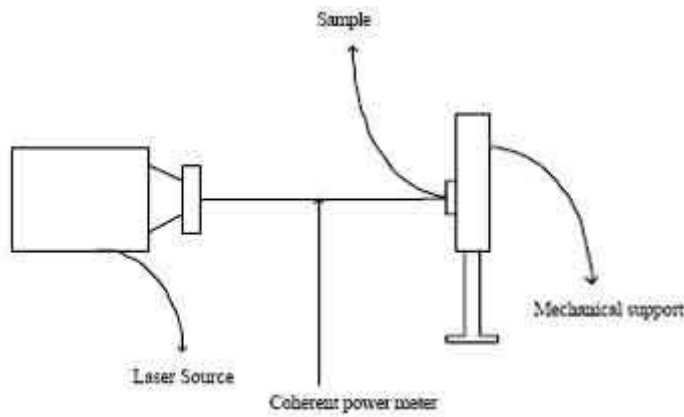


Figure 6. Experimental setup for laser experiments to characterize degradation

The laser power is measured by using a coherent power meter. The coherent meter is based on the principle of photodiodes. Each photon within the wavelength range of the device creates an electron hole pair. When reverse biased, the electron-hole pair generated results in a current flow that is proportional to the light flux. To obtain the best results the meter should be held perpendicular to the path of the laser beam. To enable measurements over a broad range of wavelengths, power levels, pulse energies and repetition rates multiple sensors can be used.

The response of the polymer sample can be categorized into, ? Initial stage (Dormant period or when there is no indication of a visual change on the surface),

- Transition stage (when the material starts vaporizing),
- Degradation stage (when a ditch is formed on the material surface).

The area of the sample that was subjected to the incident laser radiation was in the order of 200 microns and the power of the beam was in the order of 8-9 mW. Though the power density was very high any degradation that occurred in the material was not perceived by naked eye. With exposure to laser radiation there were indications of color change in the material, however, the changes were subjective. The above problem can be eliminated by using a Raman spectrometer or by increasing the area exposed to the radiation so that any deterioration in the material can be observed visually. It must be noted that the power of the laser beam cannot be increased infinitely due to practical limitations and hence any increase in the area beyond a point results in an effective decrease in the power density. The time taken to visually observe changes in the material is selected as the parameter to quantify degradation. Depth of penetration and width of the ditch produced by the beam can also be used as indicators of degradation.

Literature search shows that the depth of penetration in the material is a function of bond strength and concentration. The results reported in Table. 2 and Fig. 7 are in agreement with the theoretical conclusions. FTIR results in Fig. 4 clearly indicated a lower bond concentration and laser treatment results show a greater depth of penetration in the corona exposed region

SN	Sample	Depth of Penetration (inch)
1	Virgin silicone rubber 1 (SR1)	Negligible
2	Virgin silicone rubber 2 (SR2)	Negligible
3	Corona treated SR 1	0.065
4	Corona treated SR 2	0.049

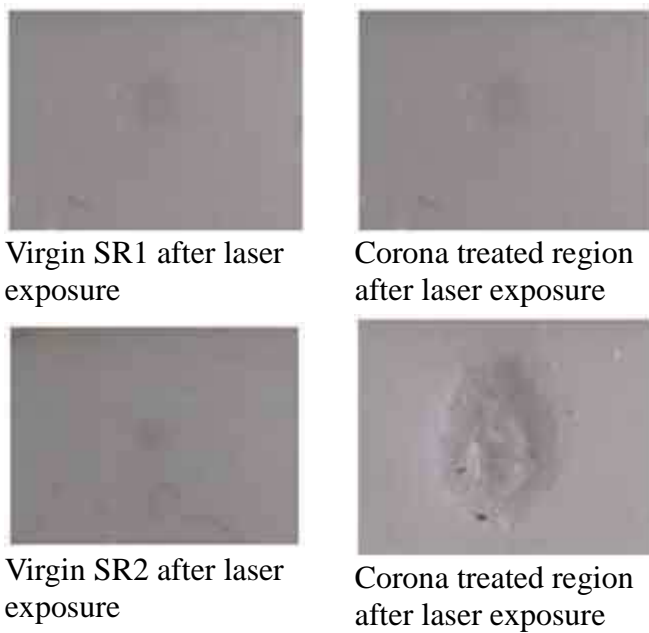


Fig 7: Depth of penetration as a function of degradation

Similar results (insignificant depth of penetration in the virgin material and the formation of a ditch in the corona exposed region) were obtained for the silicone rubber samples after recovery indicating that the laser technique could be a suitable method to characterize changes in the bulk of the material. The method can also be used to determine the energy required to cause various degrees of degradation in the material since the laser power and the time to laser exposure can be controlled.

(ii) Ethylene Propylene Diamene Monomer (EPDM)

A series of field inspections were conducted in the Phoenix metropolitan area to inspect corona occurrence on in-service insulators. An insulator (20 years field service) subjected to considerable discharge activity while in service was removed for research/experimental purposes. Corona cuts were observed on the underside of the first shed as shown in Fig. 8.

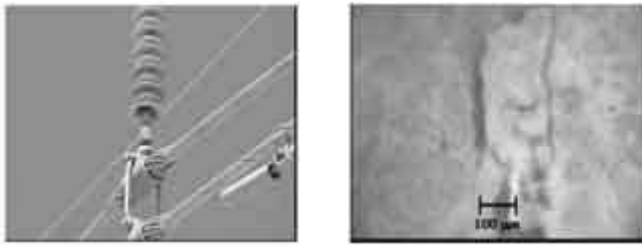


Figure 8. Corona induced degradation on a NCI (20 years field service)

A sample was cut from the shed closest to the high voltage end and FTIR analysis was performed. The region closest to the corona cut showed the maximum degradation and a decreasing trend was observed with increasing distance from the corona cut region as shown in Fig. 9.

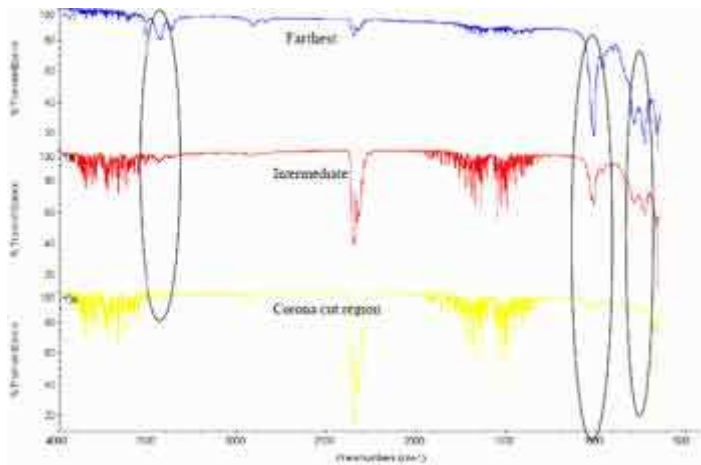


Fig 9: FTIR spectrum as a function of distance from the corona cut region

Samples from different sheds (1, 2, 3, 5, and 17) were treated with the 532 nm double YAG laser beam at 1 watt power level. The time of laser exposure was held constant (60 seconds). Samples from second shed and beyond showed little (in the form of discoloration) to no difference after laser treatment. However changes were observed along the first shed as a function of distance from the degraded region. The laser induced visual changes on the first shed is shown in Fig. 10.



Fig 10: Laser induced changes along the first shed indicated by the circles numbered 1-6

A second set of laser experiments were performed, where, time to cause a visual change was used as an indicator to degradation. The results are shown in Table. 3

S.N	Sample	Time (Sec)
1	Shed1	
	(III) In the region of corona cut	10
	(II) Intermediate region	30
	(I) Farthest from corona cut	60
2	Shed 2	63
3	Shed 3	65
4	Shed 5	64
5	Shed 17	67
6	New	120

Table 3 indicates that corona degradation in the housing material is prominent near the

high voltage end and insignificant beyond the second shed. The table further indicates sheds 2 and beyond having identical but consistently lower time to deteriorate on laser treatment when compared to the new sample (due to natural aging process).

Conclusions:

>The preliminary results from the laser experiments have been interesting. It has been shown that the time for degradation due to a constant energy laser source is a function of the corona exposure. Sheds closest to the HV end or the energized electrode tend to degrade sooner than locations further away from these regions. More research is needed to improve on the available results and to probe into the unknowns of insulator science in further detail.

References:

- [1] V. M. Moreno and R. S. Gorur, "Effect of long-term corona on non-ceramic outdoor insulator housing materials," *IEEE Trans. on Dielectrics and Electrical Insulation*, Vol. 8, No. 1, pp. 117-128, 2001.
- [2] V. M. Moreno, "Effect of long-term corona on non-ceramic outdoor insulator housing material," PhD Dissertation, Arizona State University, August 2001.
- [3] A. J. Phillips, R. H. Billings, and H. M. Schneider, "Water drop corona effects on full-scale 500 kV non-ceramic insulators," *IEEE Trans. Power Delivery*, Vol. 14, No. 1, pp. 258-265, Jan. 1999.
- [4] A. J. Phillips, D. J. Childs, and H. M. Schneider, "Aging of non-ceramic insulators due to corona from water drops," *IEEE Trans. Power Delivery*, Vol. 14, No. 3, pp. 1081-1089, July 1999.
- [5] A. A. Kulikovski, "Production of chemically active species in the air by a single positive streamer in a non-uniform Field," *IEEE Trans. Plasma Science*, Vol. 25, No. 3, pp. 439-446, 1997.
- [6] M. M. Shahin, "Ionic reactions in corona discharges of atmospheric gases," *Advances in chemistry series: Chemical Reactions in Electrical Discharges*, Vol. 80, pp. 48-58, 1969.
- [7] N. Yoshimura, S. Kumugai and S. Nishimura, "Electrical and environmental aging of silicone rubber used for outdoor insulation," *IEEE Trans. on Dielectrics and Electrical Insulation*, Vol. 6, No. 5, pp. 632-650, 1999.
- [8] V. M. Moreno and R. S. Gorur, "Ac and dc performance of polymeric housing materials for HV outdoor insulators," *IEEE Trans. on Dielectrics and Electrical Insulation*, Vol. 5, No. 3, pp. 342-350, 1999.
- [9] J. Montesinos, R. S. Gorur, B. Mobasher and D. Kingsbury, "Mechanism of brittle fracture in non ceramic insulators," *IEEE Trans. Dielectrics and Electrical Insulation*, Vol. 9, No. 2, pp. 236-243, April 2002.

- [10] A. E. Vlastos, S. M. Gubanski, "Surface Structural Changes of Naturally Aged Silicone and EPDM Composite Insulators," *IEEE Trans. on Power Delivery*, vol. 6, no. 2, pp. 888-900, April 1991.
- [11] A. R. Chughtai, D. M. Smith, L. S. Kumosa, M. Kumosa, "FTIR Analysis of Non-ceramic Composite Insulators," *IEEE Trans. on Dielectrics and Electrical Insulation*, vol. 11, no. 4, pp. 585-596, Aug. 2004.
- [12] L. Stevens, "Laser Basics," Englewood Cliffs, N. J.: Prentice-Hall, 1985.
- [13] L. H. Meyer, E. A. Cherney, S. H. Jayaram, "The Role of Inorganic Fillers in Silicone Rubber for Outdoor Insulation Alumina Tri-hydrate or Silica," *IEEE Electrical Insulation Magazine*, vol. 20, no. 4, pp. 13-21, July-Aug. 2004.
- [14] L. Meyer, S. H. Jayaram, E. A. Cherney, "Thermal Conductivity of Filled Silicone Rubber and its Relationship to Erosion Resistance in the Inclined Plane Test," *IEEE Trans. on Dielectrics and Electrical Insulation*, vol. 11, no. 4, pp. 620-630, Aug. 2004.
- [15] L. Meyer, S. H. Jayaram, E. A. Cherney, "Correlation of Damage, Dry-band Arcing Energy, and Temperature in Inclined Plane Testing of Silicone Rubber for Outdoor Insulation," *IEEE Trans. on Dielectrics and Electrical Insulation*, vol. 11, no. 3, pp. 424-432, June. 2004.
- [16] L. D. Laude, C. Cochrane, Cl. Dicara, C. Dupas-Bruzek, K. Kolev, "Excimer Laser Decomposition of Silicone," *Nuclear Instruments and Methods in Physics Research, B* 208 (2003) 314-319.
- [17] N. Arnold, N. Bityurin, D. Bauerle, "Laser-induced Thermal Degradation and Ablation of Polymers: Bulk Model," *Applied Surface Science*, 138-139 (1999) 212-217.
- [18] N. Bityurin, N. Arnold, B. Lukyanchuk, D. Bauerle, "Bulk Model of Laser Ablation of Polymers," *Applied Surface Science*, 127-129 (1998) 164-170.
- [19] Montgomery, D. C. (2004) *Introduction to Statistical Quality Edition*, New York: Wiley